J Comput Neurosci (2008) 25:262–281
DOI 10.1007/s10827-008-0077-7

Spike timing dependent plasticity promotes synchrony of inhibitory networks in the presence of heterogeneity

Sachin S. Talathi · Dong-Uk Hwang · William L. Ditto

Received: 25 July 2007 / Revised: 15 January 2008 / Accepted: 16 January 2008 / Published online: 23 February 2008

Abstract Recently Haas et al. (J Neurophysiol 96: 3305–3313, 2006), observed a novel form of spike timing dependent plasticity (iSTDP) in GABAergic synaptic couplings in layer II of the entorhinal cortex. Depending on the relative timings of the presynaptic input at time t_{pre} and the postsynaptic excitation at time t_{post}, the synapse is strengthened ($\Delta t = t_{post} - t_{pre} > 0$) or weakened ($\Delta t < 0$). The temporal dynamic range of the observed STDP rule was found to lie in the higher gamma frequency band ($\geq$40 Hz), a frequency range important for several vital neuronal tasks. In this paper we study the function of this novel form of iSTDP in the synchronization of the inhibitory neuronal network. In particular we consider a network of two unidirectionally coupled interneurons (UCI) and two mutually coupled interneurons (MCI), in the presence of heterogeneity in the intrinsic firing rates of each coupled neuron. Using the method of spike time response curve (STRC), we show how iSTDP influences the dynamics of the coupled neurons, such that the pair synchronizes under moderately large heterogeneity in the firing rates. Using the general properties of the STRC for a Type-1 neuron model (Ermentrout, Neural Comput 8:979–1001, 1996) and the observed iSTDP we determine conditions on the initial configuration of the UCI network that would result in 1:1 in-phase synchrony between the two coupled neurons. We then demonstrate a similar enhancement of synchrony in the MCI with dynamic synaptic modulation. For the MCI we also consider heterogeneity introduced in the network through the synaptic parameters: the synaptic decay time of mutual inhibition and the self inhibition synaptic strength. We show that the MCI exhibits enhanced synchrony in the presence of all the above mentioned sources of heterogeneity and the mechanism for this enhanced synchrony is similar to the case of the UCI.

Keywords Inhibitory synapses · Spike timing dependent plasticity · Synchronization · Networks · Heterogeneity

Action Editor: Carson C. Chow

S. S. Talathi (✉) · D.-U. Hwang · W. L. Ditto
J Crayton Pruitt Family Department of Biomedical Engineering, University of Florida, FL 32611, USA
e-mail: stalathi@bme.ufl.edu

D.-U. Hwang
e-mail: donguk.hwang@bme.ufl.com

W. L. Ditto
e-mail: william.ditto@bme.ufl.com

1 Introduction

It is generally accepted that inhibitory interneurons are important for synchrony in the neocortex. Several studies have reported a role for inhibitory interneurons in generating stable synchronous rhythms in the neocortex (Bernardo 1997; Jefferys et al. 1996; Michelson and Wong 1994; Whittington et al. 1995; Bragin et al. 1995). Cortical oscillations in the gamma frequency band (20–80 Hz), are thought to be involved in binding of object properties such as color and shape of a given object through synchronization, a process of great significance in the brain and its conscious perception of the surrounding world (Ritz and Sejnowski 1997).

The set of experimental findings and the importance of the binding property mentioned above has led to a

number of theoretical studies of synchrony among inhibitory interneurons (Ernst et al. 1995; vanVreeswijk et al. 1994; Wang and Rinzel 1992). The result of these studies can in general be summarized as: depending on the decay time of the inhibitory synaptic coupling, mutually coupled inhibitory neurons exhibit in-phase synchrony (zero phase difference) or out-phase synchrony (phase difference of π). However much of the above investigations did not explore the effects of heterogeneity in the intrinsic firing rates on synchronization nor did they take into account noise, which is invariably present in neuronal systems. In another set of theoretical investigations, White et al. (1998) explored the effects of small heterogeneities on the degradation of synchrony of fast spiking inhibitory neurons, and the mechanism by which the degradation occurs. They found that introduction of even small amounts of heterogeneity in the external dc current that drives the firing rate of the neuron, resulted in a significant reduction in the coherence of neuronal spiking. They attributed this loss in synchrony to the failure of a heterogeneous network to entrain the frequency of firing. It is important then to understand what mediates observed *in vivo* synchrony of inhibitory neuronal networks under biologically realistic conditions of noise induced unpredictability and intrinsic heterogeneity in the spiking rates of the neuronal ensemble.

In this paper we study the issue of sensitivity of synchrony to heterogeneity in neuronal firing rates, in the context of recently observed spike timing dependent plasticity in inhibitory synapses (iSTDP; Haas et al. 2006). We begin our analysis by considering a pair of unidirectionally coupled interneuron's (UCI) with dissimilar intrinsic firing rates. We study the influence of iSTDP on the synchronization properties of these two coupled neurons. We observe that iSTDP modulates the synaptic coupling strength such that the driven neuron fires synchronously in-phase with the driving neuron. The stability of this in-phase synchronous solution is then studied in terms of the stability of the fixed point of spike time evolution map for the coupled neurons using the spike time response method (Acker et al. 2004).

We then explore the function of iSTDP in *enhancing* synchronization between mutually coupled interneurons (MCI) with self inhibition in the presence of heterogeneity in the intrinsic firing rates. We consider the following set of heterogeneity in the MCI: (a) heterogeneity in external dc current, I^{DC}, (b) heterogeneity in the synaptic decay time, τ_D and (c) heterogeneity in the self inhibition strength, g_s.

Earlier work (Nowotny et al. 2003; Zhigulin et al. 2003) has explored the function of synaptic plasticity at an excitatory synapse in improving synchronization of a unidirectionally coupled neuronal network. They demonstrated that STDP of excitatory synapses with the property that the synaptic strength decreases when postsynaptic spike occurs after the presynaptic spike ($\Delta t = t_{\text{post}} - t_{\text{pre}} > 0$) and vice-versa, result in increased synchronization. In addition the role of gap junction coupling between interneurons in enhancement of synchronization has also been well studied (Skinner et al. 1999). It was shown in Kopell and Ermentrout (2004), that gap junction coupling plays a complementary role with respect to chemical synapses in synchrony of inhibitory neuronal network. The authors demonstrated that while, inhibition through GABAergic synapses is important for mitigating the effect of the initial conditions, it is the gap junction coupling that significantly improves synchronization in the presence of heterogeneity. *Our results in this work demonstrate that inhibitory plastic synapses can serve similar role by significantly improving synchronization in the presence of heterogeneity*.

The paper is organized as follows: In the methods section we present the mathematical model for the neuron, the synapse and the network studied. We then define the spike time response curve (STRC) for an isolated neuron with self inhibition. We then present the empirical iSTDP rule, observed by Haas et al. (2006) and use it in this paper to study the synchronization properties of the inhibitory network in the presence of heterogeneity. In the results section, we begin with the demonstration of the influence of iSTDP on synchronization of the two unidirectionally coupled interneurons. We then derive an analytic expression for the evolution of spike times for each neuron using STRC and then demonstrate how the iSTDP modulates the synaptic strength to synchronize the driven neuron to fire in-phase with the driving neuron for a broad range of heterogeneity in the firing rates. A similar enhancement in synchronization brought about by iSTDP is observed in the MCI with different intrinsic firing rates.

We have also done some investigation on the influence of noise in the presence of iSTDP on the synchronization property of the MCI. We considered two potential sources of noise through the milieu of the neuronal environment which might influence the dynamics of the network. The first source of noise considered was in the intrinsic firing frequency of each neuron and the second source of noise was considered in the modulation strength of the iSTDP. We found that even in the presence of mild noise, iSTDP plays a critical role in maintaining the synchronous state under heterogeneity. All the details on iSTDP induced

synchrony in the UCI and the MCI in the presence of noise will be presented in future work.

2 Methods

2.1 Model neuron

Each neuron is modeled based on Hodgkin Huxley framework as a single compartment model with fast sodium channel, delayed rectifier potassium channel and a leak channel. The parameters of the model are set such that it represents a cortical neuron model of type I (Ermentrout 1996). Each neuron is self inhibited through a GABAergic synaptic model which obeys second order kinetics. The dynamical equation for the model neuron is given by,

$$C\frac{dV(t)}{dt} = I^{DC} + g_{Na}m^3(t)h(t)(E_{Na} - V(t)) + g_K n^4(t)(E_K - V(t)) + g_L(E_L - V(t)) + I_M(t) + I_S(t) \quad (1)$$

where $C = 1\,\mu F/\text{cm}^2$. $V(t)$ is the membrane potential, I^{DC}: external DC current drive, is set such that the neuron spikes at a given intrinsic frequency $F(I^{DC})$. $I_S(t) = g_s S_S(t)(E_I - V(t))$, is the synaptic current due to self inhibition and $I_M(t) = g_M(t)S_M(t)(E_I - V(t))$ is the synaptic current from external inhibition. g_s is the synaptic strength of self inhibition and $g_M(t)$ is the dynamic synapse, whose strength is determined by the inhibitory synaptic plasticity rule discussed below. E_r (r = Na, K, L) are reversal potentials of the sodium and potassium ion channels and the leak channel respectively. E_I, is the reversal potential of the inhibitory synapse. g_r (r = Na, K, L) represent the conductance of sodium, potassium and the leak channel respectively.

The gating variables $X = \{m, h, n\}$ satisfy the following first order kinetic equation: $\frac{dX(t)}{dt} = \alpha_X(V(t))(1 - X(t)) - \beta_X(V(t))X(t)$, where α_X and β_X are given by

$$\alpha_m = \frac{0.32(13-(V(t)-Vth))}{e^{\frac{(13-(V(t)-Vth))}{4.0}}-1} \qquad \beta_m = \frac{0.28((V(t)-Vth)-40)}{e^{\frac{((V(t)-Vth)-40)}{5}}-1}$$

$$\alpha_h = 0.128e^{\frac{17-(V(t)-Vth)}{18}} \qquad \beta_h = \frac{4}{e^{\frac{40-(V(t)-Vth)}{5}}+1}$$

$$\alpha_n = \frac{0.032(15-(V(t)-Vth))}{e^{\frac{(15-(V(t)-Vth))}{5}}-1} \qquad \beta_n = \frac{0.5}{e^{\frac{(V(t)-Vth)-10}{40}}}$$

with $V_{th} = -65$ mV.

$S_Y(t)$, $(Y = \{S, M\})$ gives the fraction of bound receptors and satisfy the following first order kinetic equation (Abarbanel et al. 2003),

$$\dot{S}_Y(t) = \frac{S_0(\theta(t)) - S_Y(t)}{\hat{\tau}(S_I - S_0(\theta(t)))}$$

where $Y = \{S, M\}$, and $\theta(t) = \sum_i \Theta(t - t_i).\Theta((t_i + \tau_R) - t)$. $\Theta(X)$ is the heaviside function satisfying $\Theta(X) = 1$ if $X > 0$ else $\Theta(X) = 0$ and t_i is the time of the ith presynaptic neuronal spike. In the case of self inhibition the presynaptic neuron is the same as the post synaptic neuron. The kinetic equation for $S(t)$ involves two time constants, $\tau_R = \hat{\tau}(S_I - 1)$, the docking time for the neurotransmitter and $\tau_D = \hat{\tau}S_I$, the undocking time constant for the neurotransmitter binding. Finally, $S_0(\theta)$ is the sigmoidal function given by, $S_0(\theta) = 0.5(1 + \tanh(120(\theta - 0.1)))$.

In Table 1 we list all the parameters for the model considered, unless otherwise stated in the text and figure captions.

All the model parameters given above are within physiological range and give high spike rates typical of the fast spiking interneurons (Lacaille and Williams 1990; McCormick et al. 1985).

All the simulations were done using 4th order Runge–Kutta method for differential equations with time step $\delta t = 0.01$ ms, on a 2 GHz Intel Core Duo Mac OS X. The source code is available from authors on request.

2.2 Spike time response curve (STRC)

As a measure of the influence of synaptic input on the firing times of a neuron, we define the spike time response curve (STRC) $\Phi(t, \tau_R, \tau_D, g, T^0) = T - T^0$ (Acker et al. 2004; Oprisan et al. 2004), where T^0 is the intrinsic period of spiking for a given neuron model obtained by driving the neuron with a fixed DC current I^{DC} and T is the time at which the neuron fires a spike after it has received a perturbation through synaptic input at time $t < T$, in its spiking cycle. The key to the computation of STRC is that the perturbation is through a model GABAergic input with synaptic parameters, τ_R: the synapse rise time, τ_D: the synaptic decay time and g: the synaptic strength. In general this input

Table 1 List of all the parameters for the model considered

Neuron model	E_{Na}	50 mV
	E_K	−95 mV
	E_L	−64 mV
	g_{Na}	215 mS/cm^2
	g_K	43 mS/cm^2
	g_L	0.813 mS/cm^2
Synapse model	E_I	−82 mV
	g_S	0.2 mS/cm^2
	g_M (static synapse)	0.1 mS/cm^2
	τ_R	0.2 ms
	τ_D	5 ms

need not be weak. The STRC is obtained numerically here using the direct method of STRC computation as shown in the schematic diagram of STRC calculation in Fig. 1(a). The neuron firing regularly with period T^0, is perturbed through inhibitory synapse at time t after the neuron has fired a spike at reference time zero. The spiking time for neuron is considered to be the time when the membrane voltage V, crosses a threshold (set to 0 mV in all the calculations presented here). As a result of this perturbation, the neuron fires the next spike at time T which is different from T^0, the time at which the neuron would have fired a spike in absence of any perturbation through inhibitory synapse. The STRC measures this shift in firing time of the neuron $T - T^0$ as a function of the time of perturbation in the neuronal firing period through the synaptic input. As shown in Fig. 1(b) the STRC is obtained by varying the perturbation time t, over the entire cycle of

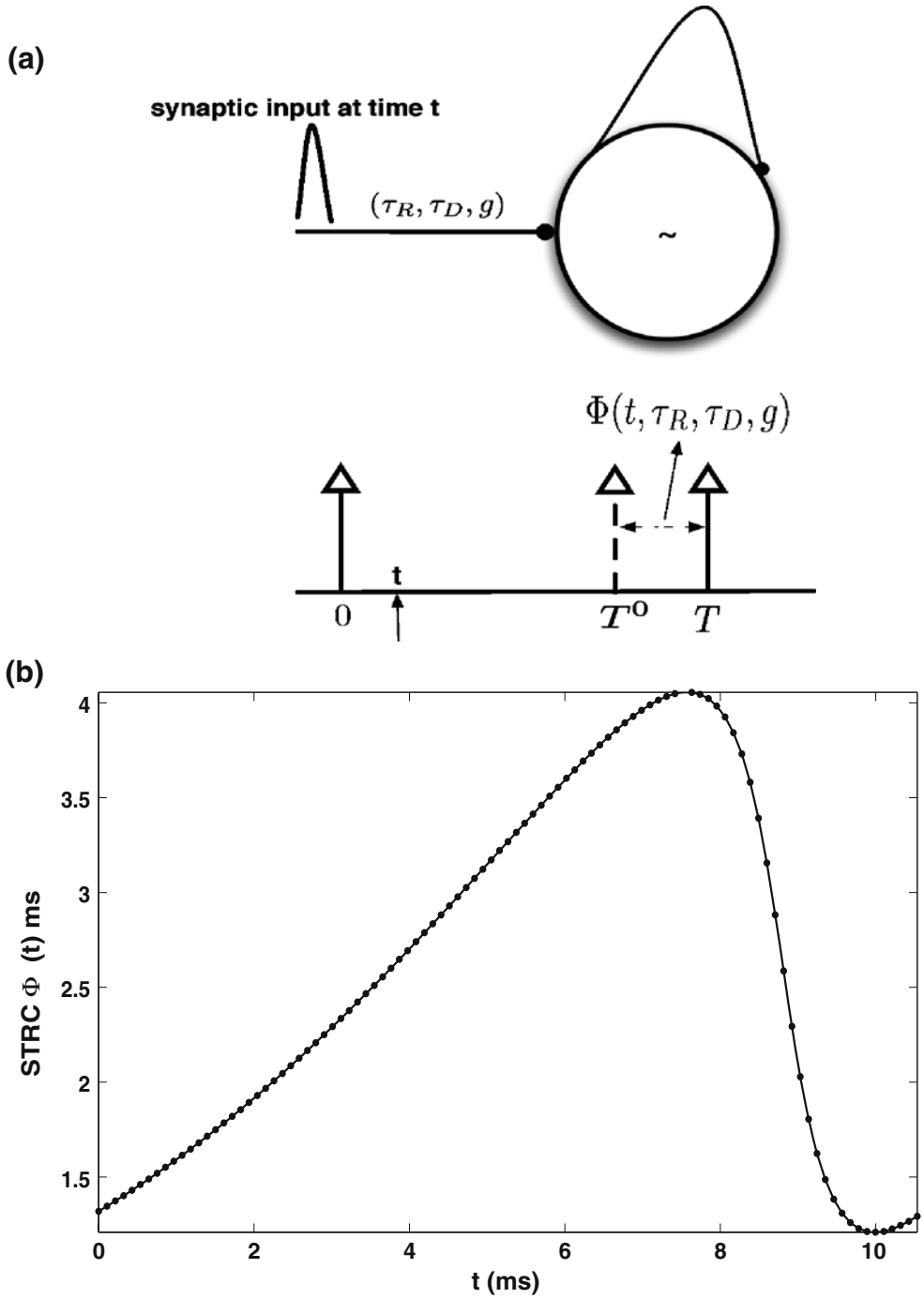

Fig. 1 Spike time response curve (STRC). (**a**) Schematic diagram demonstrating the perturbation effect of synaptic input to neuron firing at given period T^0. A perturbation is delivered to the neuron through the inhibitory synapse at time t after the last neuronal spike at reference time t. The perturbation results in the next spike of neuron occurring at time T which is different from the time of spike for neuron T^0 in the absence of any synaptic perturbation. The STRC measures this shift in spike time as function of the time t, when the perturbation is delivered (**b**) STRC of neuron firing with period $T^0 = 10.6$ ms. The synaptic parameters are: $\tau_R = 0.2$ ms, $\tau_D = 5$ ms, and $g = 0.1$ mS/cm^2

spiking ($T^0 = 10.6$ ms, for the example considered) and plotting Φ versus the perturbation time t. The synaptic parameters for computation in Fig. 1(b) are, $\tau_R = 0.2$ ms, $\tau_D = 5$ ms, $g = 0.2$ mS/cm^2 .

STRC is analogous to the phase response curve (PRC; Ermentrout 1996). Similar to the PRC for type I neurons, the STRC results in the subsequent spike of the neuron receiving an inhibitory input to be delayed in time. For brevity of notation, in all further calculations, unless otherwise mentioned, we suppress the dependence of Φ on τ_R, τ_D and define $\Phi(t, \tau_R, \tau_D, g) \equiv \Phi(t, g)$.

2.3 Spike timing dependent plasticity of inhibitory synapses

A spike timing dependent plasticity rule for inhibitory synapses (iSTDP) has been recently reported in Haas et al. (2006) and an empirical fit to the observed experimental data was obtained with the following functional form

$$\Delta g(\Delta t) = \frac{g_0}{g_{\text{norm}}} \alpha^\beta |\Delta t| \Delta t^{\beta-1} e^{-\alpha|\Delta t|} \tag{2}$$

where $\Delta t = t_{\text{post}} - t_{\text{pre}}$. t_{pre} is the time of presynaptic spike input arrival and t_{post} is the time of a spike generated by the postsynaptic neuron. g_0 is the scaling factor accounting for the amount of change in inhibitory conductance induced by the synaptic plasticity rule and is set to $g_0 = 0.02$ in all the calculations presented here. $g_{\text{norm}} = \beta e^{-\beta}$ is the normalizing constant. With parameter values $\alpha = 1$ and $\beta = 10$ (Haas et al. 2006), we obtain a window of ± 20 ms over which the efficacy of synaptic plasticity is non zero. In Fig. 2 we show the iSTDP rule fit with functional form given in Eq. (2). Four key properties of the iSTDP rule are summarized below:

1. $\Delta g(\Delta t) > 0$ for $\Delta t > 0$
2. $\Delta g(\Delta t) < 0$ for $\Delta t < 0$
3. $\Delta g(\Delta t) \approx 0$ for $\Delta t \approx 0$ and
4. $\Delta g(-\Delta t) = -\Delta g(\Delta t)$

Properties 1 and 2 above imply that a pre-synaptic spike occurring before post-synaptic excitation will always enhance the strength of inhibitory synaptic input and vice-versa. Property 3 imply that the synaptic strength of self inhibition is not modified by the spiking neuron as the pre and the post synaptic spikes for the self inhibitory synapse occur at the same time, i.e., $\Delta t = 0$. Property 4, emerges from our choice of same values for parameters α and β for both positive and negative Δt regions. We have also explored the effect of asymmetry

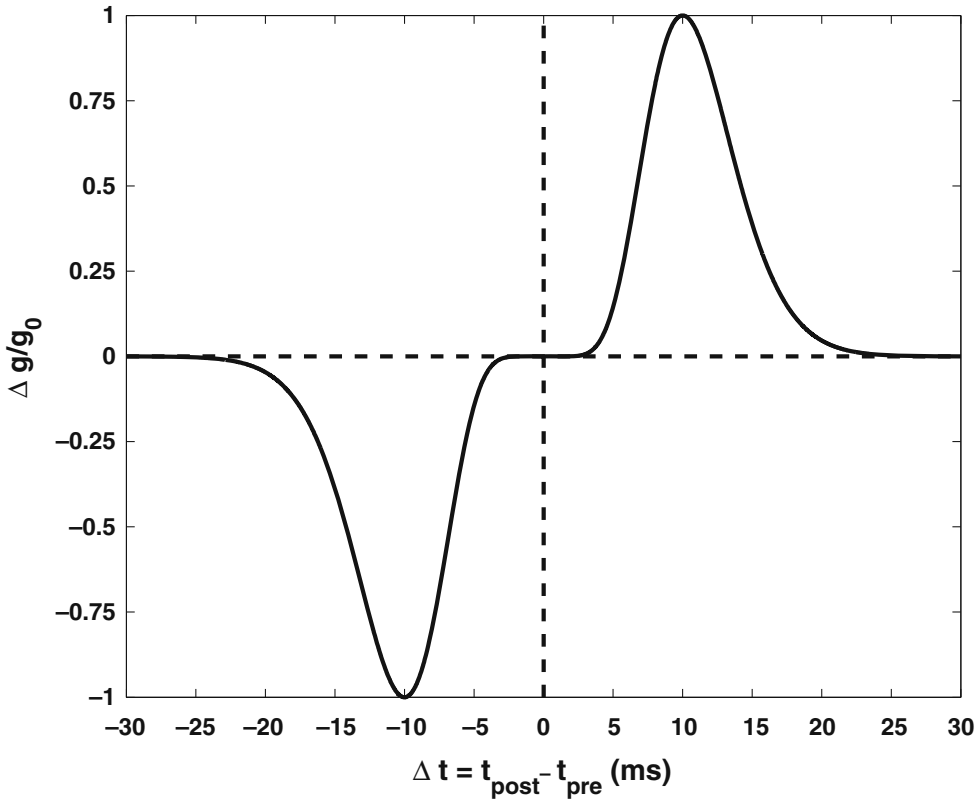

Fig. 2 STDP rule for inhibitory synapses. The parameters are $\alpha = 1$, $\beta = 10$ and $g_0 = 1$

in the empirical rule on the synchronization properties of the inhibitory network. We find that for level of asymmetry as presented in Haas et al. (2006), where for $\Delta t > 0$, $\alpha = 0.94$ and for $\Delta t < 0$, $\alpha = 1.1$, with $\beta = 10$, the enhancement in synchronization window through iSTDP remains essentially the same as presented in Fig. 6. In all the calcutions presented in this work, unless otherwise mentioned, the parameters for the empirical fit for iSTDP define in Eq. (2) are, $\alpha = 1$, $\beta = 10$ and $g_0 = 0.02$.

2.4 Inhibitory neuronal network

We consider a network of two neurons with self inhibition in (a) unidirectional coupling and (b) bidirectional coupling (mutual inhibition), configuration as shown in Fig. 3. Synchronization in the case of unidirectional coupling requires that the driven neuron (1) fires at a higher rate as compared to the driving neuron (2) because the effect of inhibition is to slow the firing rate of the inhibited neuron.

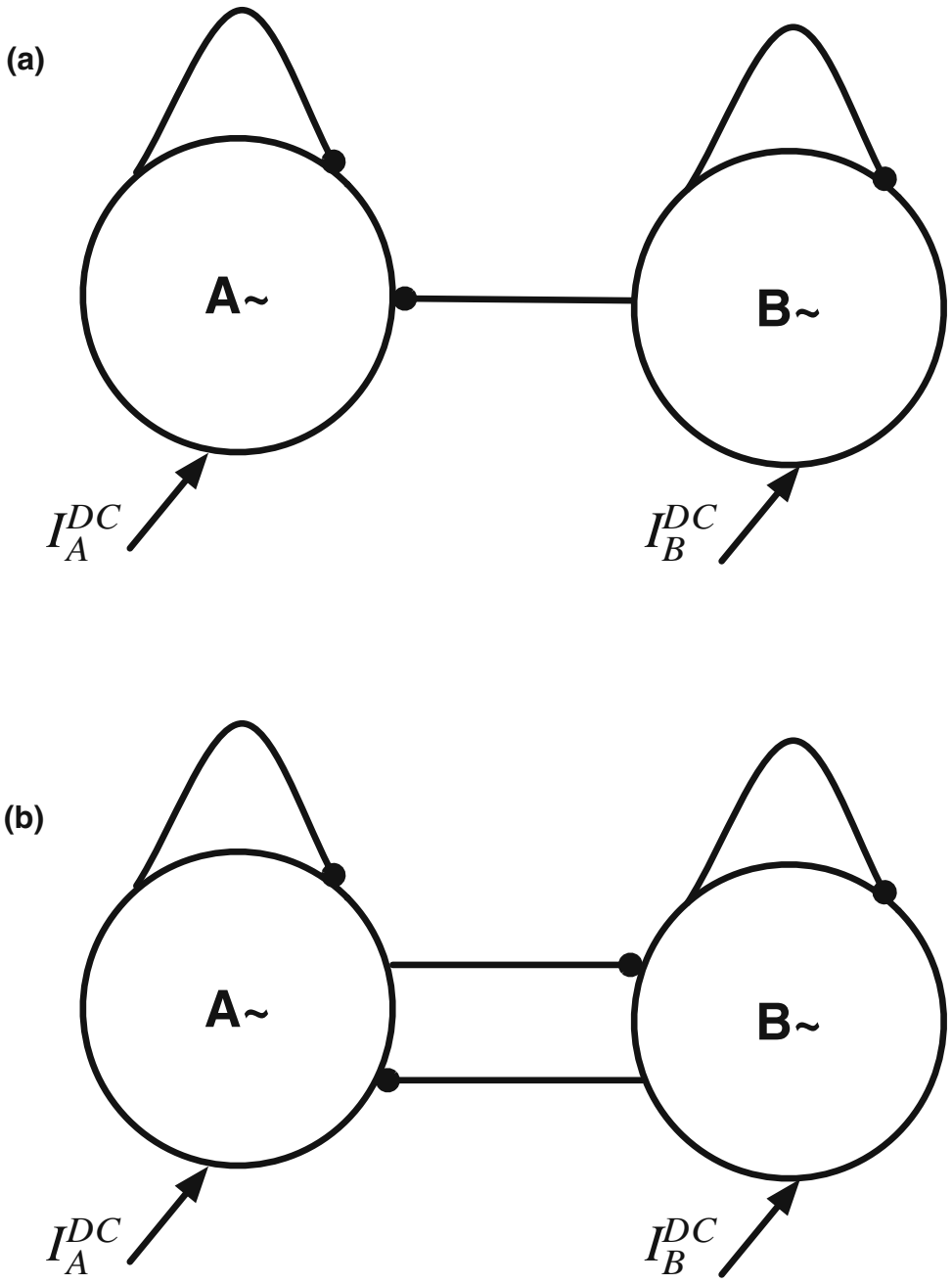

Fig. 3 Inhibitory neuronal network. (**a**) Unidirectional coupled interneurons (UCI), $I_{DC}^A > I_{DC}^B$; (**b**) mutually coupled interneurons (MCI), $I_{DC}^A \neq I_{DC}^B$. The $\sim$ in $(K \sim)$, $K \equiv \{A, B\}$, represents the fact that the strength of constant input drive I^{DC} is such that each neuron is driven above the threshold for spiking and has an intrinsic firing rate $F(I^{DC})$

3 Results

3.1 Single self inhibited neuron

We begin with the study of the firing characteristics of single self inhibited neuron dependent on the synaptic parameters: the rise time τ_R, the decay time τ_D and the strength of self inhibition, g_s. Spike based adaptation, dependent on self inhibition is considered for the following reasons,

- Biological neural networks often have local inhibitory interneurons which deliver feedback inhibition to the cells that activate those interneurons (Sheperd 1990).
- It has been shown by Traub et al. (2001), that the frequency in the gamma regime in a distributed network of inhibitory interneurons is highly dependent on synaptic decay time. This effect has been simulated through self inhibition in our model.
- The iSTDP learning rule considered in this work, has a zero at $\Delta t = 0$, which implies, the strength of self inhibition is not modulated through the iSTDP rule. As a result, the synchronization in the UCI and the MCI, is not modulated by changes in self-inhibition strength of through iSTDP. In addition, self-inhibition provides a control over frequency range of operation of the neuron through the synaptic parameters.

In Fig. 4, we show the frequency response of the neuron for the following set of synaptic parameters, $g_s = \{0.2, 0.5, 0.75, 1.0\}$ mS/cm^2, $\tau_R = \{0.1, 0.5, 1.1, 2.0\}$ ms and $\tau_D = \{5, 10, 25, 50\}$ ms. We see that while the biologically realistic time scales for synaptic rise time do not have a significant effect on the firing characteristics of the self inhibited neuron, the synaptic decay time and the strength of self inhibition do significantly decrease the firing frequency of the neuron for a fixed level of input drive I^{DC}. This results from the fact that for slower synaptic decay times the effect of inhibition persists longer. As a result the neuron takes longer time to recover from hyper-polarization to produce a spike again. Also if the strength of inhibition is high, the neuron is strongly inhibited and it takes a longer time to recover back to produce the next spike. Thus τ_D, the decay time of self inhibition and g_s, the synaptic strength of self inhibition determines the frequency regime of operation of the neuron. Heterogeneity in one of these parameters will significantly affect the synchronization properties of network of inhibitory neurons.

3.2 Spike time scheme for the analysis of iSTDP induced synchrony

For the analysis of iSTDP induced synchrony in the UCI and the MCI in the presence of heterogeneity using STRC, we adopt the following representation for spike times from neuron A and B:

Let $W_A = [w_A(1), w_A(2), \cdots w_A(i), \cdots w_A(N_A)]$, where $w_A(i) = t_A^i$ and t_A^i represents the time of ith spike from neuron A and N_A is the total number of spikes from neuron A. Similarly we define the set $W_B = [w_B(1), w_B(2), \cdots w_B(j), \cdots, w_B(N_B)]$ with $w_B(j) = t_B^j$, where t_B^j again represents the time of jth spike from neuron B. We now define a new set W_E comprising of all spike times from the coupled system (UCI/MCI) arranged in monotonically increasing order as follows, $W_E = W_A \oplus W_B = [w_E(1), w_E(2), \cdots w_E(N_A + N_B)]$. For example, if $t_A^1 < t_B^1 < t_A^2$, the first two elements in the set W_E are, $w_E(1) = t_A^1$ and $w_E(2) = t_B^1$ respectively. In the case when neurons A and B fires at the same time, we have for some i, and j, $t_A^i = t_B^j$. These two simultaneous spike events are added to W_E such that, for some n, $w_E(n) = t_A^i$ and $w_E(n+1) = t_B^j$. We next define two new sets, $\widetilde{W}_A$ and $\widetilde{W}_B$, which represents a modified spike time series for neurons A and B defined by, $\widetilde{W}_{A/B} = [\tilde{w}_{A/B}(1), \tilde{w}_{A/B}(2), \cdots \tilde{w}_{A/B}(N_A + N_B)]$,where each element $\tilde{w}_{A/B}(n)$ is obtained from $W_{A/B}$ and W_E as follows,

$$\tilde{w}_{A/B}(n) = \max\left(w_{A/B}(i) \le w_E(n)\right) \quad \left(0 < i \le N_{A/B}\right)$$

We now define an inter spike interval (ISI) time series $s(n)$, for the coupled system as $s(n) = w_E(n+1) - w_E(n)$. When the two neurons show in-phase synchrony with period T, we have $s(2n-1) = 0$ and $s(2n) = T$, $\forall\, n > 0$. For the case of dynamic synapse, the synaptic strength $g(t)$ is modulated by the pre-post synaptic spike pairs through iSTDP [Eq. (2)]. We define $g(t) = g(n)$ when $w_E(n) \le t < w_E(n+1)$. In Fig. 5 we show the schematic diagram for the spike time scheme used for the analysis of the iSTDP induced synchrony as presented in this section.

3.3 iSTDP induced synchrony in the UCI

3.3.1 Numerical simulations

We consider two self inhibited neurons with unidirectional coupling [Fig. 3(a)] in the presence of heterogeneity in their intrinsic firing rates introduced through

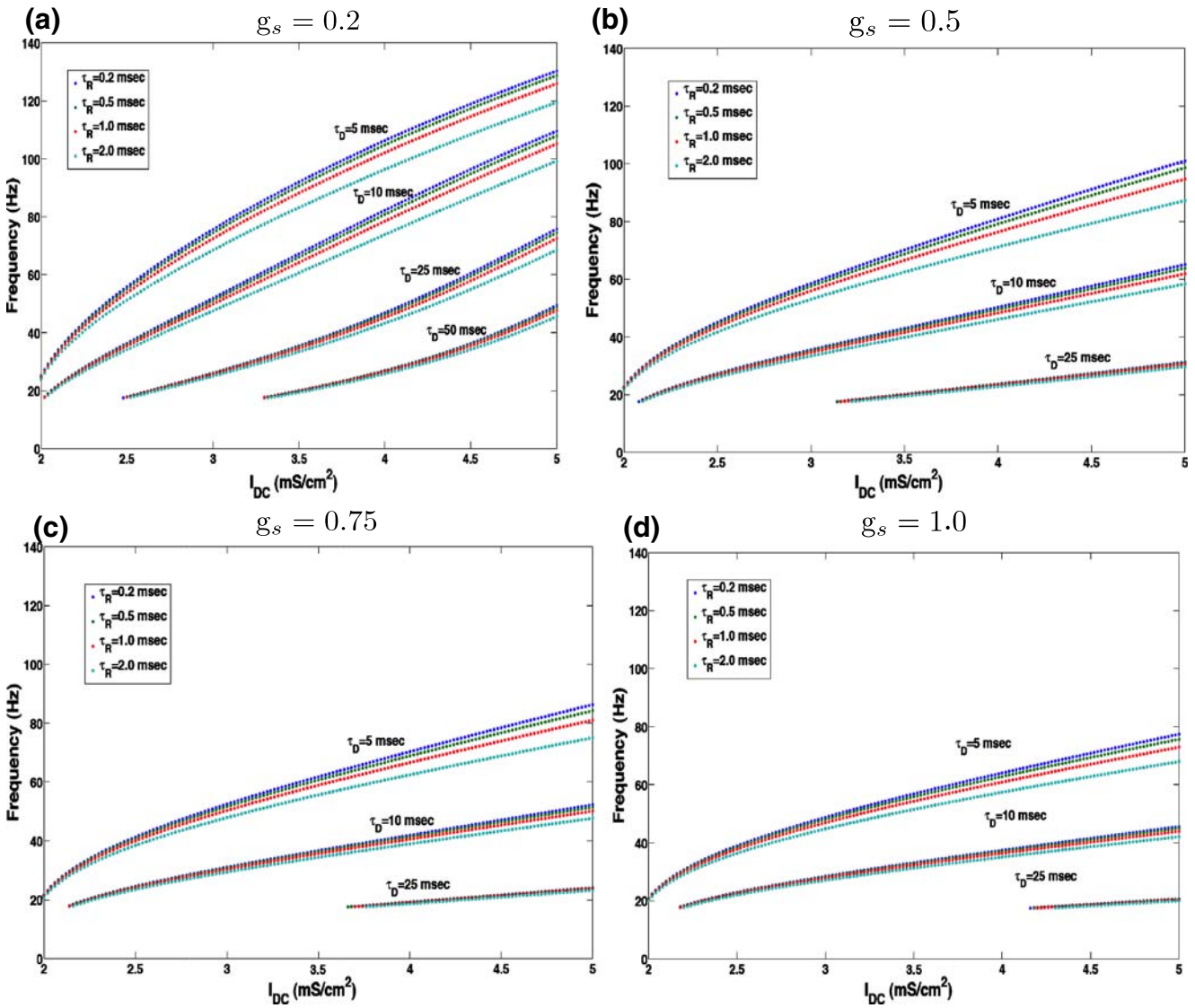

Fig. 4 Frequency response of single self inhibited neuron as function of the input current I^{DC}, for given synaptic parameters of self inhibition: The synaptic decay time τ_D, The synaptic rise time τ_R and the strength of self inhibition g_s. In each case,{a,b,c,d} all the parameters for neuron model are constant, however we vary the strength of self inhibition as, g_s={0.1,0.5,0.75,1.0} mS/cm^2 respectively. See online publication for the color version of this figure

different external drive (I^{DC}) and study the synchronization properties of the coupled neurons in the context of dynamic synapse. We set $I_B^{DC} = 2.5$ μA/cm^2, such that neuron B is firing at frequency of $F(I_A^{DC}) =$ 56 Hz, giving an intrinsic period of $T_B^0 \approx 17.85$ ms. We define heterogeneity

$$H = 100\frac{I_A^{DC} - I_B^{DC}}{I_A^{DC} + I_B^{DC}}$$

where I_A^{DC} is the steady input current in neuron A. When $I_A^{DC} \approx I_B^{DC}$, the heterogeneity $H \approx 0$ and if all other neuronal parameters are identical, the two neurons have identical firing rates. For $I_A^{DC} \gg I_B^{DC}$, $H \approx$ 100 and the two neurons are maximally heterogeneous in terms of their firing rates. For all the simulations below, unless otherwise mentioned, the initial conditions on the membrane potentials, $V_A(t = 0) = -75$ mV and $V_B(t = 0) = -65$ mV. We have also run numerical simulations for a number of different initial conditions on the membrane potential and found that the iSTDP induced synchronous state is the global attractor of the coupled system. Also, all the spike times required by the synaptic update rule and the STRC calculations were obtained as the time when the membrane voltage of neuron rose through a threshold of 0 mV.

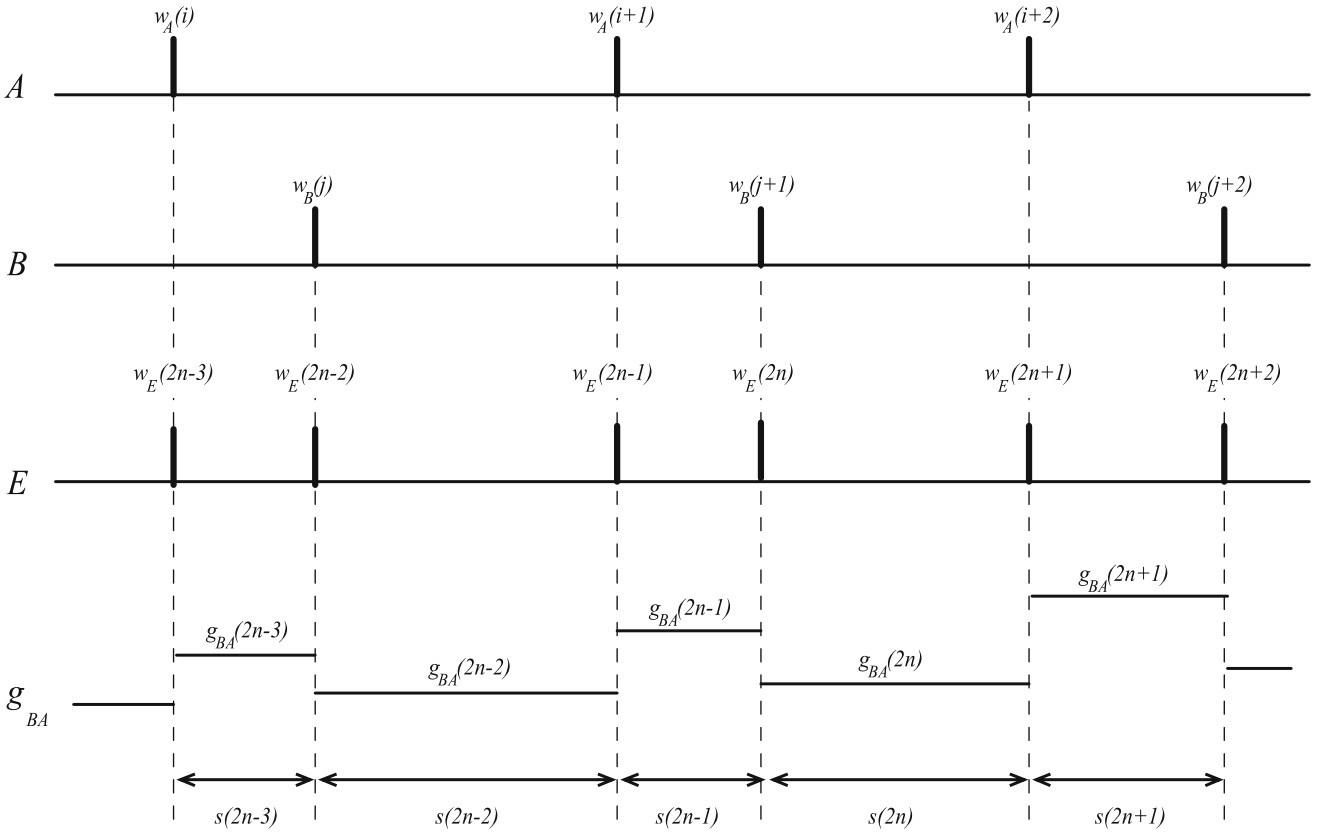

Fig. 5 The set W_A. W_B, W_E corresponding to the spike times of neuron A, neuron B and the coupled system are shown. We also show the inter-spike interval s between the spikes in the coupled system and the evolution of the dynamic synapse g_{BA} modulated by the iSTDP rule

We now consider two situations: one in which the conductance of the inhibitory synapse from B to A, g^S_{BA} is static, with $g^S_{BA} = 0.1$ mS/cm^2 (g_{ij} is the conductance of inhibitory synapse from neuron i onto neuron j), and a second situation in which the inhibitory synaptic strength is dynamic and is governed by the iSTDP rule given in Fig. 2, such that

$$g_{BA}(n) = g_{BA}(n-1) + \Delta g(\tilde{w}_A(n) - \tilde{w}_B(n)) \tag{3}$$

where $g_{AB}(n)$ is synaptic strength from B to A for duration, $w_E(n) \leq t < w_E(n+1)$ (see Results, Section 3.2).

In defining the synaptic update rule defined above, we make two key assumptions

- The iSTDP update is considered to be dependent only on the two nearest spike neighbors, and the effects of spike pairs is assumed to sum linearly, following the conditions under which (Haas et al. 2006) experimentally observed the iSTDP. We ignore multi-spike interactions, which have been shown to play a significant role in STDP of excitatory synapses (Froemke and Dan 2002) and also any dependence of iSTDP on the frequency of firing of the pre-synaptic neuron.
- The iSTDP update is assumed to happen instantaneously, as a result we ignore the delay that exists between the pairing of the pre and post-synaptic spikes and the resultant induction of synaptic modification as suggested by the experiments.

The implication of above assumptions regarding the iSTDP update rule, are explored in more details in the discussion section. We begin with the initial synaptic strength $g_{BA}(t=0) \equiv g_{BA}(0) = g^S_{BA} = 0.1$ mS/cm^2. In order to determine synchrony in the firing of the UCI, in Fig. 6(a) we plot the ratio of the period for spiking for neuron B (the driver neuron) T^0_B to the average period for spiking for neuron A, $\langle T_A \rangle$ as a function of heterogeneity H, for the two cases considered above: Static synapse, and Dynamic synapse, modulated by iSTDP rule defined in Eq. (2). We see that in the case of static synapse, neuron B is able to entrain neuron A to fire at its frequency for mild levels of heterogeneity H (from about 2 to 12). But as the heterogeneity increases beyond $H \approx 12$, neuron B with a static synapse is no

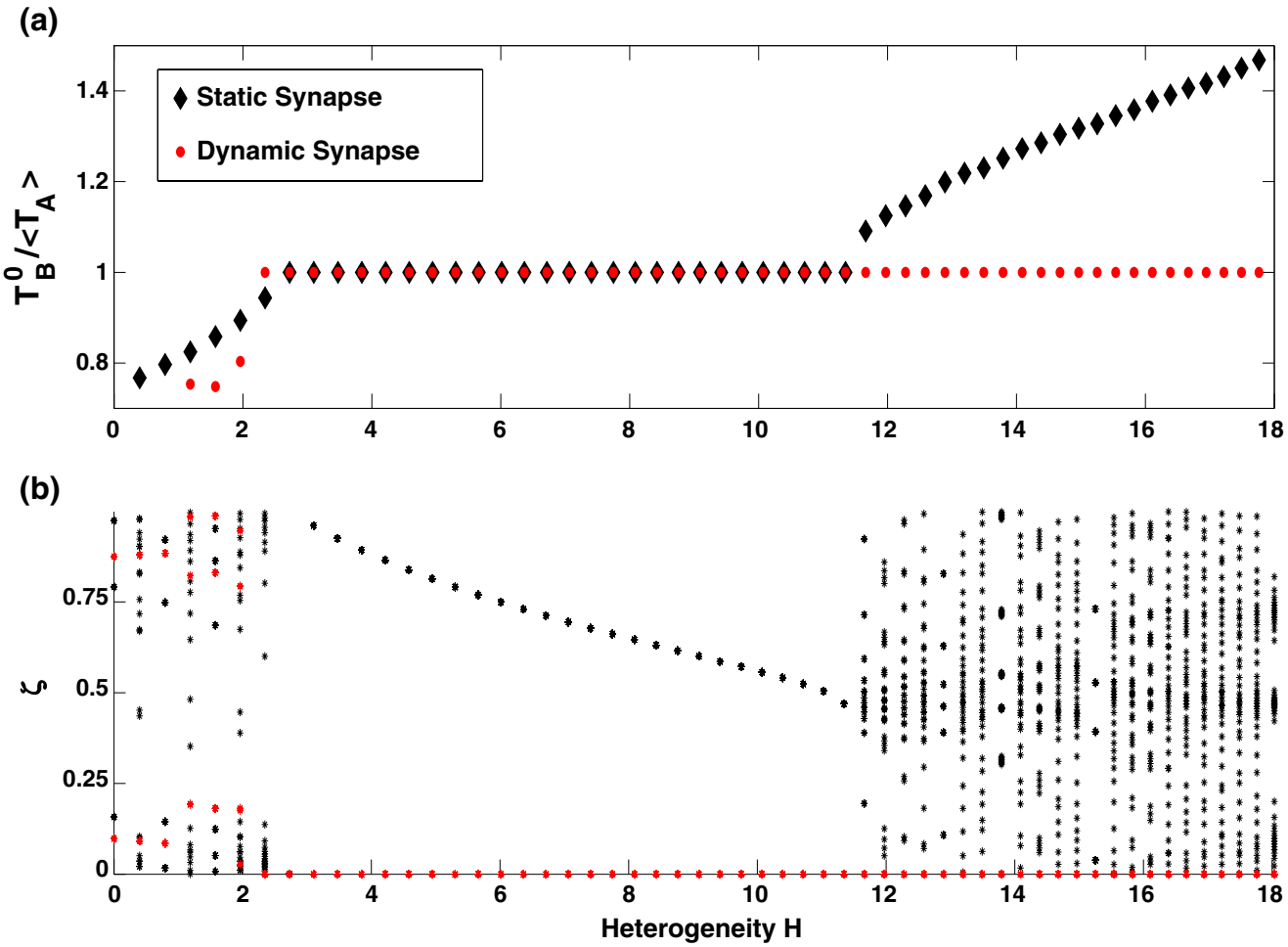

Fig. 6 Synchronization in the UCI with static (*black*) and dynamic synapse (*red*). (**a**) The ratio of average spiking period of each neuron of the UCI is plotted as function of heterogeneity H. (**b**) The generalized phase difference ζ is plotted as function of heterogeneity H. See online publication for the color version of this figure

longer able to entrain neuron A to fire at its frequency and the two neurons fire asynchronously.

In Fig. 6(b), we show the scatter plot of the phase difference, $\zeta(n)$, between the two coupled neurons as function of heterogeneity H. We define the general phase difference $\zeta(n)$ at $w_E(n)$ as

$$\begin{aligned}\zeta(n) &= \frac{w_A(i)-w_B(j)}{w_B(j+1)-w_B(j)} \\ &\quad \text{with } (w_B(j) \le w_A(i) = w_E(n) < w_B(j+1)) \\ &= \frac{w_B(j)-w_A(i)}{w_A(i+1)-w_A(i)} \\ &\quad \text{with } (w_A(i) \le w_B(j) = w_E(n) < w_A(i+1)). \quad (4)\end{aligned}$$

For the case of the UCI, Fig. 3(a), $\langle T_B \rangle = T_B^0$. We see that in the static synaptic case, the two neurons phase lock in 1:1 synchrony, with a finite phase difference ζ for a certain range of heterogeneity values ($2 < H < 12$). However with dynamic synapse, the region of 1:1 synchrony is enhanced to cover a larger range of heterogeneity and in addition, for the set of synaptic parameters considered, the two neurons always exhibit in-phase synchrony, i.e., $\zeta = 0$. As an example of such a scenario, we show in Fig. 7(a) the time series of membrane voltage of the two neurons firing asynchronously for heterogeneity of $H = 12.28$ ($I_A^{DC} = 3.2\ \mu\text{A/cm}^2$ and $I_B^{DC} = 2.5\ \mu\text{A/cm}^2$).

In the case of dynamic synapse, iSTDP is able to modulate the synaptic strength g_{BA}, such that even for increasing heterogeneity in firing frequency of neuron A, neuron B is still able to entrain the driven neuron A, to fire synchronously with neuron B. iSTDP modulates the synaptic strength to a final stable configuration at which the two neurons fire in-phase, resulting in $\tilde{w}_A(n) - \tilde{w}_B(n) \approx 0$. The particular form of the iSTDP rule ($\Delta g(\Delta t = 0) = 0$) then implies that the synaptic strength no longer changes and the network reaches a

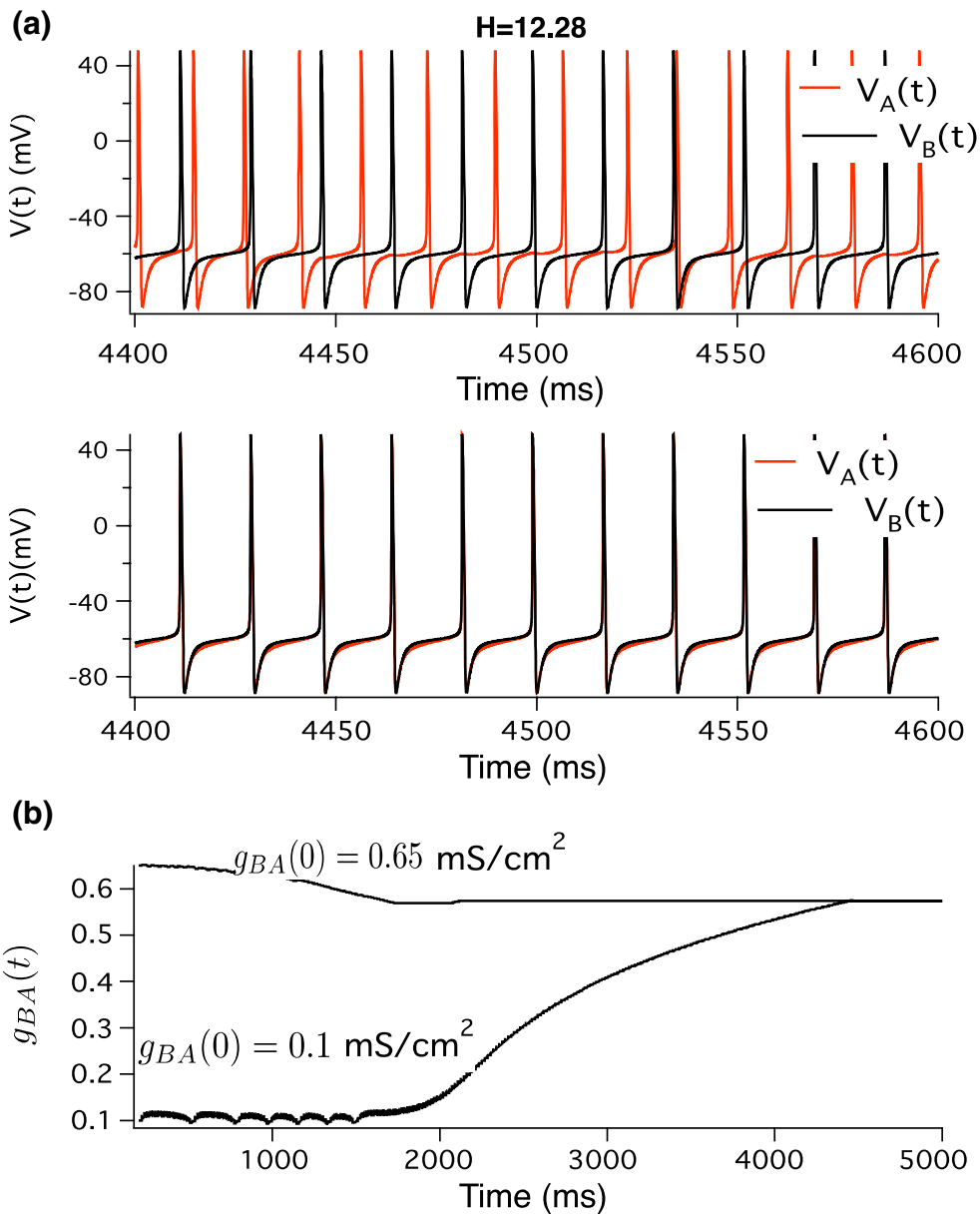

Fig. 7 (**a**) The time series of each neuron in the UCI is plotted for a given level of heterogeneity, $H = 12.28$ in the intrinsic drive I^{DC} to each neuron with (**a**) static synapse and (**b**) dynamic synapse, modulated through iSTDP. (**c**) The plot of evolution of the dynamic synaptic strength to final steady state configuration for a given heterogeneity $H = 12.28$, starting from two different initial conditions, $g_{BA}(0) = 0.1$ and $g_{BA}(0) = 0.65$ mS/cm^2 respectively. See online publication for the color version of this figure

final stable state when the two neurons are entrained to fire synchronously. In Fig. 7(b) we show the time evolution of membrane voltage of the two neurons A and B, firing synchronously in-phase for heterogeneity of H=12.28, when the inhibitory synaptic strength has evolved to a final steady state configuration. In Fig. 7(c) we show an example of evolution of the inhibitory synaptic strength through iSTDP from two different initial conditions to final steady state configuration, resulting in the in-phase synchrony of the UCI. Note that for initial strength $g_{BA}(0) = 0.1$ mS/cm^2, the synaptic strength oscillates around this value for a long time until eventually it monotonically increases to the final steady state value at which the two neurons are locked in in-phase synchrony. The oscillation in synaptic strength and the monotonic increase further on, represent two distinct states of the UCI which will be explored in details below.

3.3.2 Stability analysis of UCI synchrony by STRC

In order to understand the mechanism of synchrony in the UCI we use the method of STRC to derive a map for the evolution of the time difference $s(n)$. In order to simplify the analysis we assume that the two neurons fires alternatively, specifically neuron A fires at

$t_E(2n-1)$, while neuron B fires at $t_E(2n)$, $\forall\ n > 0$. For a given fixed inhibitory synaptic strength, g^S_{BA}, if $\Phi_A(t, g_{BA})$ is the STRC for neuron A, we have (Fig. 5)

$$\begin{aligned} w_E(2n+1) - w_E(2n-1) &= T^0_A + \Phi_A\big(w_E(2n) \\ &\quad - w_E(2n-1), g^S_{BA}\big) \\ &= T^0_A + \Phi_A\big(s(2n-1), g^S_{BA}\big) \end{aligned} \tag{5}$$

Also by definition of $s(2n)$, we have

$$\begin{aligned} w_E(2n+1) - w_E(2n-1) &= (w_E(2n+1) - w_E(2n)) \\ &\quad + (w_E(2n) - w_E(2n-1)) \\ &= s(2n) + s(2n-1). \end{aligned} \tag{6}$$

Similarly, since neuron B fires with period of T^0_B, we have

$$s(2n+1) + s(2n) = T^0_B \tag{7}$$

Then from Eqs. (5), (6) and (7), we have

$$s(2n+1) = T^0_B - T^0_A - \Phi_A\left(s(2n-1), g^S_{BA}\right). \tag{8}$$

The steady state solution to above equation can be obtained by solving for the fixed point s^* of odd sequence of the evolution map for $s(2n+1)$, defined by $s(2n+1) = s(2n-1) = s^*$. We then obtain

$$\Phi_A\left(s^*, g^S_{BA}\right) = T^0_B - T^0_A \tag{9}$$

The stability of the fixed point s^* requires, $0 < \frac{d\Phi(t,g)}{dt}|_{t=s^*} < 2$. In Fig. 8(a), we show the STRC for neuron A in the static synapse case with $g^S_{BA} = 0.1$ mS/cm^2 for heterogeneity $H = 12.28$ ($I^{DC}_A = 3.2$ and $I^{DC}_B = 2.5$ μA/cm^2). For this case, with the static strength of mutual inhibition set at $g^S_{BA} = 0.1$ mS/cm^2, Equation (9) has no solution since there is no intersection between the STRC $\Phi_A(t, g^S_{BA})$ and the line $T^0_B - T^0_A$, as can

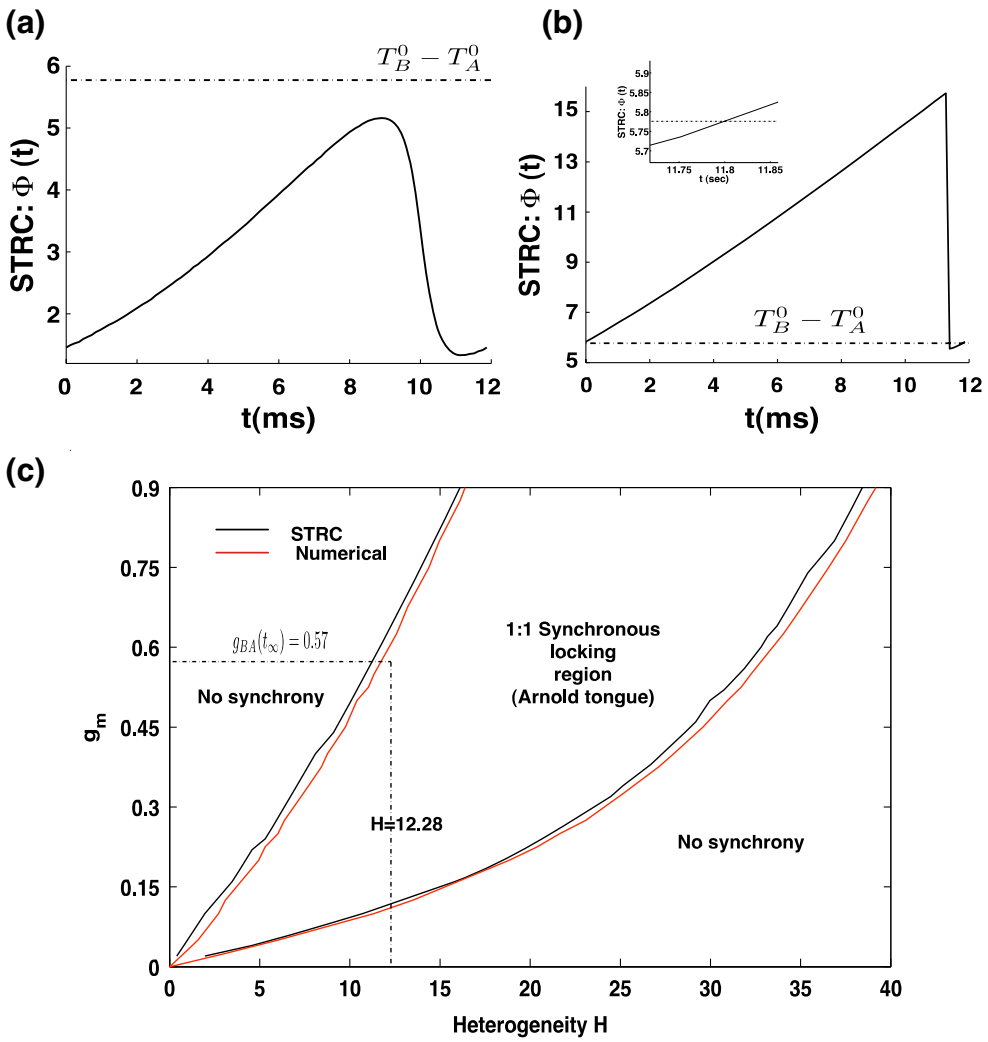

Fig. 8 (**a**) The STRC for neuron A, when the strength of synaptic inhibition $g_{BA} = 0.1$ mS/cm^2. (**b**) The STRC for neuron A, when the strength of the synaptic inhibition $g_{BA} = 0.57$ mS/cm^2, representing the final steady state value when the two neurons in the UCI are locked in in-phase synchrony. (**c**) The 1:1 synchronous regime for the UCI s determined through STRC (*black*) and numerical simulations of the model for the UCI (*red*). See online publication for the color version of this figure

be seen from Fig. 8(a) and therefore the two neurons cannot lock in synchronous state.

In Fig. 8(b), we similarly show the STRC computed with dynamic synapse in the asymptotic state when the system has locked into in-phase synchronous solution and the inhibitory synaptic strength $g_{BA}(t)$ has reached a final stable value, $g_{BA}(t=\infty) \equiv g_{BA}(\infty) = 0.57$. We see that the solution to Eq. (9) exists as the STRC curve $\Phi_A(t, g_{BA}(\infty))$ intersects the line $T_B^0 - T_A^0$ at $s^* = 11.8$ and the condition for stability for this fixed point is also satisfied.

In above example we considered a specific example for the synaptic strength, $g_{BA} = 0.1$ mS/cm^2 and determined that the lack in the existence of stable fixed point solution to Eq. (9), results in the absence of synchrony between the firing of the two coupled neurons in the UCI. We also showed that iSTDP modulated synaptic strength in the asymptotic state ($g_{BA}(\infty) = 0.57$ mS/cm^2) provides a unique stable solution to the Eq. (9), and the two coupled neurons in the UCI fire in in-phase synchrony.

3.3.3 Arnold tongue of UCI

We next solve Eq. (9) for different levels of heterogeneity H, thereby modulating T_A^0 to determine the set of inhibitory synaptic strength g_{BA} which will result in unique stable solution for Eq. (9) to exist. The solution to Eq. (9) is obtained by estimating the STRC using the direct method for STRC computation as explained in the methods section, for each value of the inhibitory synaptic strength g_{BA}, and determining, whether there exists a stable fixed point solution to Eq. (9). In Fig. 8(c) we present the results of these calculations. For given H, the curve in black gives the lower and upper bound on the set of inhibitory synaptic strengths, for which a unique stable solution for Eq. (9) exists. For example with H=10, the range of values for g_{BA} which result in an unique stable solution to exist for Eq. (9) is $0.09 < g_{BA} < 0.49$. For this range of values for inhibitory synaptic strength g_{BA}, at $H = 10$ the driver neuron B is able to entrain the driven neuron A to oscillate in synchrony with it. This region of synchronous 1:1 locking between the two coupled neurons is analogous to the classical Arnold tongue (Kurths et al. 2001) obtained for synchrony between two coupled nonlinear oscillators. Arnold tongues are typical signature of synchrony in coupled nonlinear oscillators. In general the width of synchrony between two heterogeneous neural oscillators (heterogeneity in intrinsic firing period of the oscillators) is dependent on the strength of coupling between the driver and the driven oscillator. Arnold tongues provide a two dimensional visualization of this dependence of the width of synchrony on the strength of coupling between the two oscillators. Naturally in the absence of any coupling the two oscillators are firing at their intrinsic oscillation frequency and the width of synchrony is zero. As the strength of coupling is increased, the width of synchrony increases, resulting in an tongue shaped two dimensional area. In Fig. 8(c), this general feature of Arnold tongue is represented by the area bounded by the two black curves, obtained through STRC by solving Eq. (9) as discussed above.

In Fig. 8(c), shown in red is a similar bound on the levels of heterogeneity leading to synchronous oscillation in the UCI, obtained by numerically integrating Eq. (1), for the dynamics of evolution of the two coupled neurons. The curves in red are obtained by fixing the firing period of the driver neuron B at T_B^0 and varying the intrinsic firing period for neuron A, T_A^0 by changing the dc current I_A^{DC}, thereby varying the level of heterogeneity H in the firing of the two coupled neurons, and then determining the synaptic strength g_{BA}, that will result in $\frac{T_B^0}{<T_A>} \approx 1$, so that the two neurons are locked in 1:1 synchrony. We find the results of numerical simulation match the results from STRC calculations in Fig. 8(c). We also see that for $H = 12.28$, the asymptotic value $g_{BA}(t)$ obtained through the modulation of the synapse from B to A through iSTDP is $g_{BA}(\infty) = 0.57$ mS/cm^2 which is in the region of 1:1 synchrony for the two coupled neurons. We therefore conclude that iSTDP modulates the synaptic strength g_{BA} such that Eq. (9) is satisfied and the two coupled neurons lock into 1:1 synchronous in-phase oscillation.

3.3.4 In-phase synchrony in the UCI induced by iSTDP

iSTDP however not only modulates $g_{BA}(t)$ such the two neurons are locked in 1:1 synchrony, but the strength is modulated such that the two neurons exhibit in-phase synchrony with the phase difference ζ being identically zero irrespective of H and initial $g_{BA}(0)$, as can be seen from Fig. 6(b). In order to understand the function of iSTDP in producing this in-phase synchrony between the two coupled neurons, we consider the following two scenarios with the case, $H = 12.28$ and $g_{BA}(0) = 0.1$ mS/cm^2 as an example. The initial strength of g_{BA} is outside and below the region of 1:1 synchronous locking for the two coupled neurons for given heterogeneity, as can be seen in Fig. 9.

In this situation, with $H > 0$, neuron A is firing at a higher rate than neuron B. Therefore more often than not, neuron A will fire more than once for every period of firing of neuron B. Each firing of neuron A (the postsynaptic neuron), results in corresponding increase in synaptic strength g_{BA} through iSTDP. For

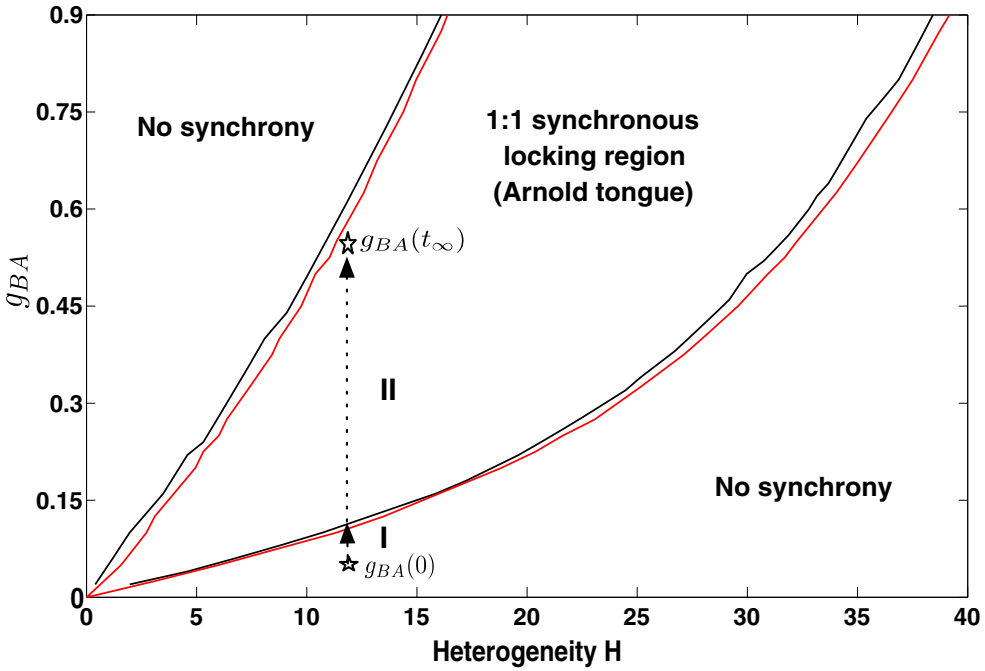

Fig. 9 Path to 1:1 in-phase synchrony. Modulation of synaptic strength to go from non-synchronous region to the Arnold tongue (I) and further modulation of the synapse to lead to stable in-phase synchrony (II). See online publication for the color version of this figure

every spike of neuron B, however only the last spike of neuron A will contribute to the decrease in the synaptic strength g_{BA} through iSTDP. This is because we consider only the nearest spike pair interaction in updating the synaptic strength at any given point in time. Overall, however with $H > 0$ and g_{BA} outside the Arnold tongue region, the probability of firing of neuron A is greater than that of neuron B and the synapse from g_{BA} increases in strength approaching the Arnold tongue from below.

In order to understand the evolution of the synaptic strength g_{BA} from a value inside the Arnold tongue to the final stable fixed point $g_{BA}(\infty)$ (Fig. 9), by iSTDP, we derive a two dimensional map for the evolution of synaptic strength and the time lag between the firing of the two neurons. Under the assumption that once the synapse have evolved to the region within the Arnold tongue, the two neurons are phase locked in synchrony, i.e., $\langle T_A \rangle \approxeq T_B^0$ and the locked state remains quasi-static as the synaptic strength evolves, the map for evolution of the quasi-static stable state s^* is obtained from Eq. (9) as,

$$\begin{aligned}
&\Phi_A\left(s^*(2n+1), g_{BA}(2n+1)\right)\\
&\quad = T_B^0 - T_A^0 \implies s^*(2n+1)\\
&\quad = (\Phi_A)^{-1}\left(T_B^0 - T_A^0, g_{BA}(2n+1)\right) \qquad (10)
\end{aligned}$$

The synaptic strength $g_{BA}(n)$ is modulated through iSTDP every time a spike event occurs either from neuron A or from neuron B. According to the iSTDP update rule as given in Eq. (3) we have,

$$\begin{aligned}
g_{BA}(2n+1) &= g_{BA}(2n) + \Delta g(\tilde{w}_A(2n+1) - \tilde{w}_B(2n+1))\\
&= g_{BA}(2n-1) + \Delta g(\tilde{w}_A(2n) - \tilde{w}_B(2n))\\
&\quad + \Delta g(\tilde{w}_A(2n+1) - \tilde{w}_B(2n+1))\\
&= g_{BA}(2n-1) + \Delta g\left(w_E(2n-1) - w_E(2n)\right)\\
&\quad + \Delta g(w_E(2n+1) - w_E(2n))\\
&= g_{BA}(2n-1) - \Delta g(s^*(2n-1)) + \Delta g(s^*(2n))\\
&\approx g_{BA}(2n-1) - \Delta g(s^*(2n-1))\\
&\quad - \Delta g(s^*(2n-1) - T_B^0)\\
&\equiv g_{BA}(2n-1) + G_{\text{eff}}(s^*(2n-1), T_B^0) \qquad (11)
\end{aligned}$$

where $G_{\text{eff}}(s, T) = -\Delta g(s) - \Delta g(s - T)$, combines the effect of spike times of each neuron A and B in modulating the synaptic strength through iSTDP.

In deriving Eq. (11), we have used the assumption of the quasi-stationarity of the locked state of the time lag s^* inside the Arnold tongue, resulting in $s^*(2n) \approx T_B^0 - s^*(2n-1)$, which results in the period of oscillation of neuron A being the same as that of the period of firing of neuron B.

Equations (10) and (11), thus give a recursive map for the evolution of the synaptic strength $g_{BA}(2n+1)$ and the time lag, $s^*(2n+1)$ between the spiking of the two coupled neurons, after the synaptic strength has evolved to a value inside the Arnold tongue. Starting

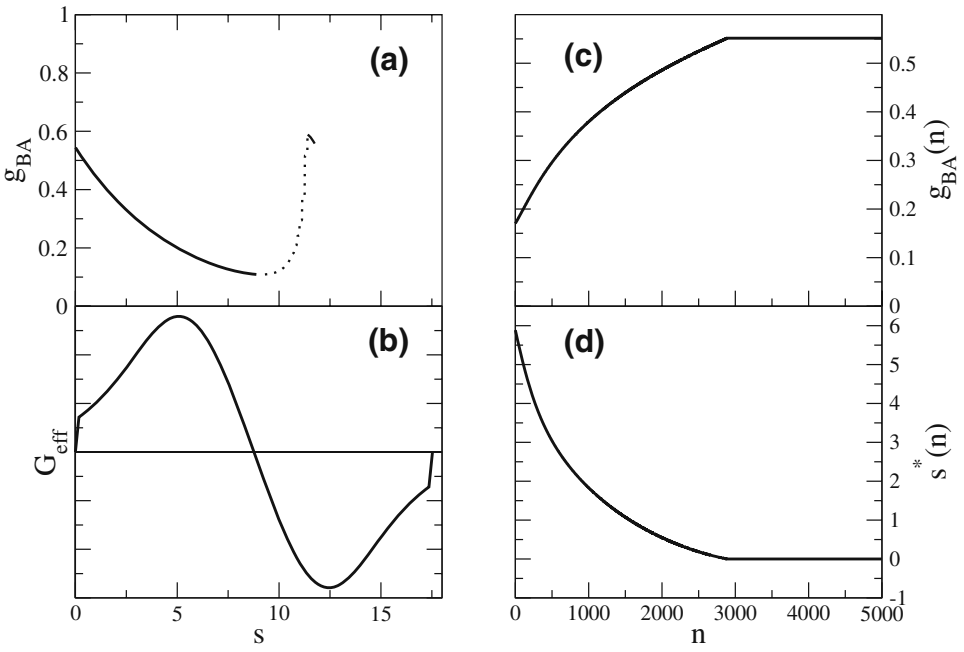

Fig. 10 Two dimensional map for the evolution of the synaptic strength within the Arnold tongue: (**a**) g_{BA} vs stable (*solid*) and unstable (*dotted*) fixed points s. (**b**) G_{eff} as a function of s. (**c**)and (**d**) shows temporal evolution of $g_{BA}(n)$ and $s^*(n)$ for the UCI with heterogeneity $H = 12.28$

from initial condition $g_{BA}(1)$ and $s^*(1)$, from Eq. (11), we determine $g_{BA}(3)$. Using the value of $g_{BA}(3)$, in the function Φ_A^{-1}, we determine $s^*(3)$ and so on.

In Fig. 10(a) and (b), we show $(\Phi_A)^{-1}$ and G_{eff} for the case $H = 12.28$. $(\Phi_A)^{-1}$ was obtained numerically from the set of STRC curves (Φ_A) computed for various s^* and g_{BA}. For given g_{BA}, we located s^* where the curve $\Phi_A(s^*, g_{BA})$ intersects line $T_B^0 - T_A^0$ by using linear interpolation. We found that there are always one stable and one unstable root, if there is intersection between $\Phi_A(s^*, g_{BA})$ and the line $T_B^0 - T_A^0$. We can therefore numerically find $(\Phi_A)^{-1}$ for stable and unstable s^* separately. In Fig. 10(a) we show, for given g_{BA}, where these stable and unstable s^* are located.

For a given $T_B^0 - T_A^0$, as g_{BA} increases due to iSTDP, the amplitude of STRC increases, as can be seen from Fig. 8(a) and (b). The solution to Eq. (10) then appears through saddle node bifurcation resulting in synchronous locking of the two coupled neurons at a stable time lag s^*. This is shown in Fig. 10(a). Once the two neurons are locked in 1:1 synchrony with a stable time lag, s^*, as we can see from Eq. (11), and Fig. 10(b), the synaptic strength g_{BA} increases resulting in a new stable state s^*, until recursively reaching the final asymptotic state of 1:1 in-phase synchrony with s^* identically zero. As the two neurons fire in-phase the synaptic strength no longer evolves and the coupled neurons are locked in 1:1 in-phase synchrony. Figure 10(c) and (d) shows the recursive evolution in the synaptic strength g_{BA} and the corresponding evolution of the time lag s^*, as given from Eqs. (10) and (11) to the final asymptotic values, $s^* = 0$ and $g_{BA}(t = \infty) = 0.57$ mS/cm^2.

It should be noted that the convergence to 1:1 synchrony between the two coupled neurons comes from generally observed properties of synchrony between two coupled oscillators and the convergence to stable in-phase synchrony are the consequence of global properties of iSTDP and the STRC for the type I neuron model considered.

3.3.5 Synchrony in the UCI and dependence on initial synaptic strength

The analysis presented above began with the assumption of the initial coupling strength $g_{BA}(0)$ being below the Arnold tongue for given heterogeneity levels considered. In such situations, in general the neuron A is firing at frequency greater than neuron B and as mentioned earlier, the synapse g_{BA} will on average increase in strength such that the synaptic strength evolves to the domain of Arnold tongue. However, if we begin with initial condition $g_{BA}(0)$ outside and above the Arnold tongue, the situation might be different. For example, for given heterogeneity level, and the initial synaptic strength outside and above Arnold tongue, the synapse might be able to modulate the firing rate of neuron A, enough such that the neuron A might fire at the same rate of neuron B or might even fire slowly. The synaptic strength according to the iSTDP rule might then evolve such the synapse might not enter 1:1 locking region at

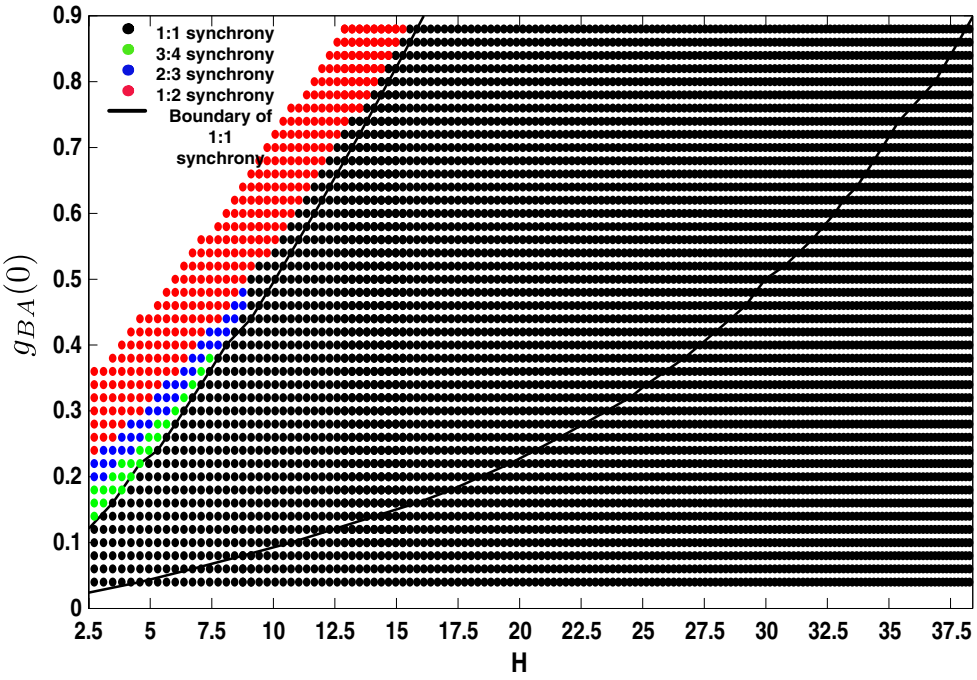

Fig. 11 Steady state reached by the UCI through the dynamic modulation of the synaptic strength, as function of the initial synaptic strength $g_{BA}(0)$ for given heterogeneity H. See online publication for the color version of this figure

all. In order to understand the evolution of dynamics under these conditions, in Fig. 11 we plot the ratio of $T_B^0/ < T_A >$ for the two coupled neurons, in the dynamic case, for a given initial strength of $g_{BA}(0)$ and given heterogeneity H.

We can see from Fig. 11, as predicted by our theoretical analysis with the two dimensional coupled map above, for all initial levels of synaptic strength below or within the Arnold tongue the coupled system evolves to 1:1 in-phase synchrony. However for initial levels of synaptic strength outside and above the Arnold tongue, we see that the system evolves in general to p:q (p,q ϵ $\mathbb{Z}$) synchrony. In addition we can also see from Fig. 11 that for low levels of heterogeneity, if the initial synaptic strength is too high neuron B inhibits neuron A from firing and no synchrony results.

3.4 iSTDP induced synchrony in the MCI

We next consider the network of two self inhibited neurons mutually coupled to each other through inhibition [Fig. 3(b)]. It has been shown earlier by White et al. (1998), that such a network with identical properties can synchronize in-phase for entire range of parameters I^{DC}, τ_D, for a given fixed value of self inhibition. However, the synchronization fails if one introduces slight heterogeneity in the firing of the two coupled neurons.

We examine this particular scenario as presented above for unidirectional coupling, in the context of dynamic synapse. We consider heterogeneity introduced through different external drive (I^{DC}), through different decay time of synaptic inhibition (τ_D) and finally through different strength of self inhibition g_s. We again compare the two situations: static synapse synchrony versus dynamic synapse synchrony. For static case we set, $g_{AB}^S = g_{BA}^S = 0.1$ mS/cm^2. For the case of dynamic synapse we have, $g_{BA}(n) = g_{BA}(n-1) + \Delta g(\tilde{w}_A(n) - \tilde{w}_B(n)))$ and $g_{AB}(n) = g_{AB}(n-1) + \Delta g(\tilde{w}_B(n) - \tilde{w}_A(n)))$. We again consider only the nearest neighbor interaction in modulating the synaptic strength. In Fig. 12(a) we plot the ratio of the average firing period of neuron B, $< T_B >$ to that of neuron A, $< T_A >$ as function of heterogeneity H introduced through different external drive, for the static and the dynamic synapse case. We see that the dynamic synaptic modulation by STDP results in p:q (p,q ϵ $\mathbb{Z}$) for all heterogeneity levels considered. In particular we see an enhanced window of 1:1 and 2:1 synchronization induced by dynamic synapse as seen in Fig. 8(b). This implies an increased probability of observing coherence in the firing pattern of the MCI even in presence of mild heterogeneity as has been reported in many *in vivo* experimental data (Eckhorn et al. 1988; Gray et al. 1989). In Fig. 12(b), we again show the scatter plot of the general phase difference ζ, as defined in Eq. (4). We again see that STDP modulates the synaptic strength such that the two neurons, either phase lock with zero phase lag (in the case of 1:1 synchrony) or the phase

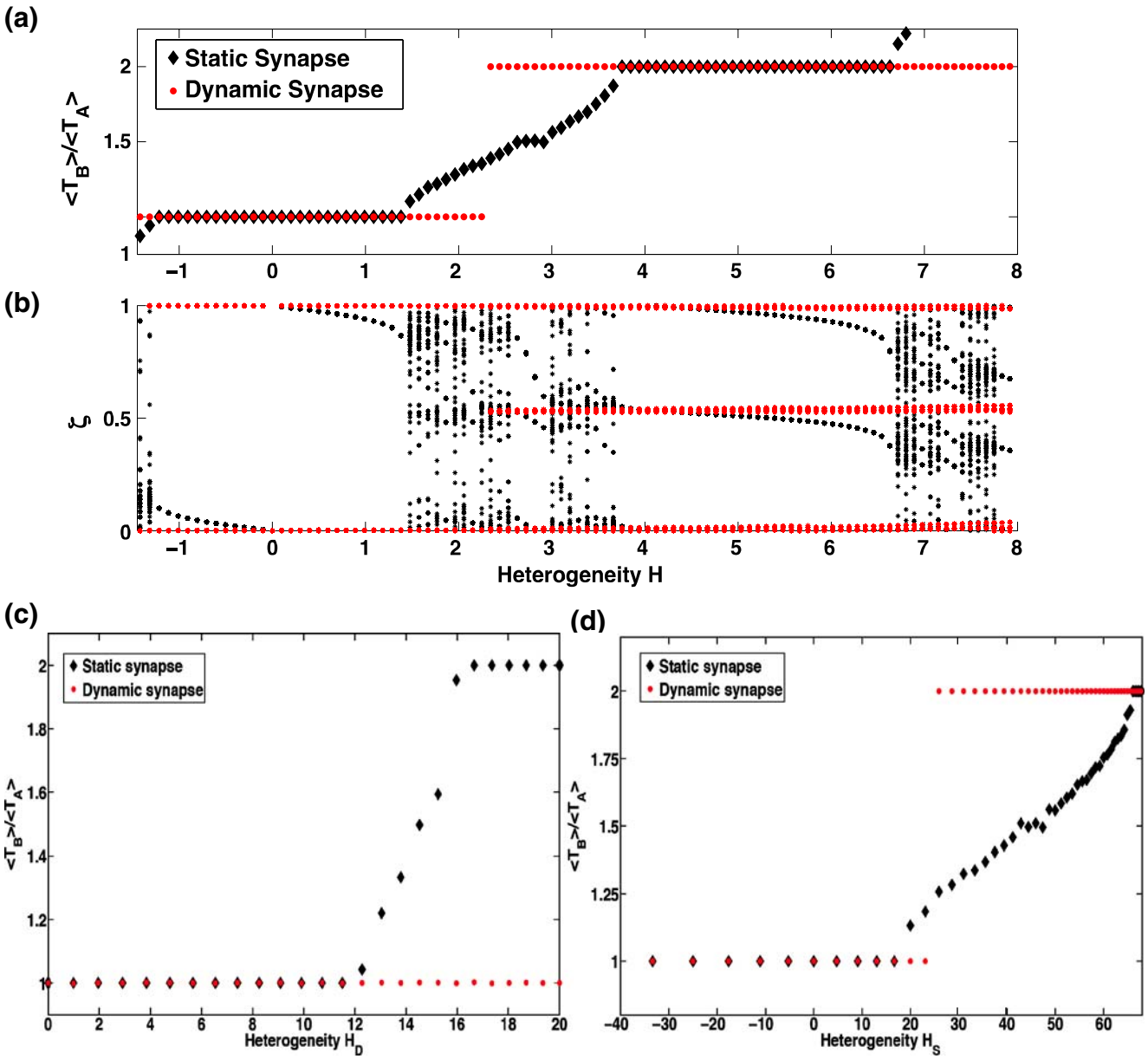

Fig. 12 Synchronization between pair of self inhibited neurons with mutual inhibition. (**a**) Heterogeneity is introduced through different input drive I^{DC}. (*1*) gives the ratio of average firing period of the two coupled neurons as function of heterogeneity H, for the case with static (*black*) and dynamic (*red*) synapse. (*2*) gives the plot of general phase difference ζ for the MCI as function of heterogeneity H. (**b**) The ratio of average firing period of the two coupled neurons in the MCI is plotted as function of heterogeneity H_S introduced through different level of self inhibition on the neurons. (**c**) The ratio of average firing period of the two coupled neurons in the MCI is plotted as function of heterogeneity introduced through different synaptic time constant τ_D. See online publication for the color version of this figure

difference oscillates between antiphase and in-phase synchrony, (2:1 frequency locking).

In Fig. 12(c), we plot the ratio of firing period of the two coupled neurons, as function of heterogeneity introduced through different synaptic decay time of the inhibition. For the results presented in this figure, we set $I_A = I_B = 2.5\ \mu\text{A/cm}^2$, $g_s = 0.1\ \text{mS/cm}^2$, the decay time for inhibitory synapse from B to A, $\tau_D^{BA} = 5$ ms and we define heterogeneity in synaptic decay time as

$$H_D = 100\frac{\tau_D^{AB} - \tau_D^{BA}}{\tau_D^{AB} + \tau_D^{BA}}$$

(τ_D^{ij} is the synaptic decay time for synapse from neuron i to neuron j). Heterogeneity in firing rate of the two

neurons is introduced by different synaptic decay time as, larger the decay time of synapse, longer is the inhibition and the neuron tends to fire at slower rate. We again see that the dynamic synapse is able to modulate the strength of inhibition on each neuron, such that the two neurons are able to synchronize over a broader range of heterogeneity in the synaptic decay time.

We finally consider a source of heterogeneity introduced by different self inhibition strength g_s. We define heterogeneity in self inhibition

$$H_S = 100\frac{g_S^B - g_S^A}{g_S^B + g_S^A}$$

The parameters for the MCI in this configuration are, $I_A^{DC} = I_B^{DC} = 2.5$ μA/cm^2, $\tau_D = 5$ ms, $\tau_R = 0.1$ ms and $g_S^A = 0.1$ mS/cm^2. In Fig.12(d), we show the results comparing synchrony between the two coupled neurons with static synapse and dynamic synapse. Again the coupled neurons with dynamic synapse show a greater robustness in synchrony as compared to the static case.

In order to understand synchrony in the MCI, with dynamic modulation of both synaptic strength g_{AB} and g_{BA}, we numerically simulated the MCI with the evolution rule applied to the synapse from slower firing neuron B to the faster firing neuron A, g_{BA} as in the unidirectional case studied above, and fixed the synaptic strength in opposite direction g_{AB} fixed at moderately lower strength. Depending on the initial condition on the synaptic strength g_{BA}, the two neurons either phase locked in in-phase 1:1 synchrony or the system evolved to 2:1 synchrony. We thus conclude that synchrony in the MCI is brought about by the modulation of the synapse from the slower neuron to the faster neuron and that the modulation in the synapse from faster neuron to the slower neuron, simply controls the firing rate of the slower neuron and prevents the effective inhibition of the slower neuron by the faster neuron.

4 Discussion

In this work we have analyzed the functional significance of spike timing dependent plasticity, recently observed for inhibitory synapses (Haas et al. 2006) in synchronizing a pair of neurons with self inhibition in two coupling configurations: (a) uni-directional coupling and (b) bi-directional coupling. We begin with the study of a single self inhibited neuron and show how the firing frequency of the neuron is dependent on the decay time of the synapse and the strength of the self synapse. Slower synaptic decay time results in prolonged influence of inhibition and it takes longer time for neuron to recover from inhibition to fire again, there by decreasing the firing frequency of neuron for the same level of input drive through I^{DC}. The presence of self inhibition which results in spike based adaptation in firing of the neuron was considered because it has been shown that the frequency in the gamma band in a distributed network of inhibitory neurons is highly dependent on the synaptic decay time. This effect can be simulated through self inhibition. Moreover the iSTDP learning rule, considered in this study has an interesting zero at $\Delta t = 0$ implying that iSTDP does not modulate the self inhibition synaptic strength. Thus the analysis of synchrony through STRC is unaffected by the presence of self inhibition. In addition (as can be seen from results in Section 3.1) the parameters of the self inhibition synapse, provide control over the frequency range of the operation of the neuron and provide an additional source of heterogeneity that might influence synchrony between mutually coupled interneurons.

Network of mutually coupled neurons with intrinsic heterogeneity in firing frequency has been studied earlier in White et al. (1998). These authors demonstrated that even a mild introduction of heterogeneity in the network results in disruption of synchrony in the network as the coupling not only has to align the phase for synchrony but also has to entrain the frequency of firing of the two neurons. They showed that synchrony is achieved only when inhibition is strong enough so that the firing period is dominated by the synaptic decay time. However a very strong inhibition results in loss of synchrony through suppression whereby the faster spiking neuron inhibits the slow neuron so much so that it stops firing.

In this work we show that a possible route to achieve stable synchronous oscillations in the presence of heterogeneity is through spike timing dependent plasticity of inhibitory synapses. Recently Haas et al. (2006), have reported spike timing dependent plasticity of inhibitory synapses (iSTDP) in layer II of the entorhinal cortex. In this work we have utilized the functional form for this recently observed synaptic plasticity rule to study its influence on the synchronization of inhibitory neuronal network in the presence of heterogeneity. The empirical fit to iSTDP data observed by Haas et al. (2006), is presented in Fig. 2. We have shown that in the presence of heterogeneity, the dynamic synapse through iSTDP results in significant enhancement of neural synchrony. The iSTDP modulates the synaptic strength such that the faster spiking neuron slows down through increase in inhibition on it and vice versa. We would like to

note that STDP of inhibitory synapses has also been observed in acute hippocampal slices (Woodin et al. 2003). The authors report a functional form for iSTDP in hippocampal slices that is symmetric with respect to the timing of the pre- and postsynaptic spikes and is non-zero at zero time delay, which is distinctly different from the functional form for iSTDP rule observed in the entorhinal cortex by Haas et al. (2006). The significance of this form of iSTDP in the enhancement of synchrony in inhibitory neuronal network remains to be explored.

In all our calculations for the dynamic modulation of the inhibitory synaptic strength and the theoretical analysis thereof, we have made two key assumptions for the update rule governed by iSTDP. We considered only the neighboring spike pair interaction for iSTDP and assumed that the effect of the iSTDP modulation sum linearly. This assumption allowed us to obtain an analytic expression for the evolution of the synaptic strength, after the two coupled neurons are phase locked and have evolved to the region within the arnold tongue. It has also been shown by Froemke and Dan (2002), that in the presence of natural spike trains, the contribution to synaptic modification is primarily through the timing of the first spike in each burst. It would be interesting to see how the dynamics of synchrony between the MCI would be affected through such multi-spike interaction. The second key assumption we made was that the iSTDP update happens instantaneously, thereby we ignore the actual delay of several minutes that exists between the pairing of the pre and post-synaptic spikes and the results induction of synaptic modification. Although our assumption of instantaneous iSTDP update implies that the synaptic modification has time scale much faster than the firing rate of the neuron, which is contrary to the observed experimental results, the mere introduction of delay in synaptic update, as seen in experiments, has no consequence for our results. In order to verify that it is indeed the case, we varied the intensity of change in synaptic strength through iSTDP by modulating g_0, such that the increment in the synaptic strength induced by iSTDP is much smaller in the UCI. We observed no changes in the results from our simulations.

In Fig. 6 we compared the synchrony in the UCI with heterogeneity in the presence and absence of dynamic synapse. We see that iSTDP results in 1:1 synchrony between the two neurons for all levels of heterogeneity considered. We analyzed this network synchrony with the method of STRC and demonstrate that iSTDP modulates the synaptic strength such that there exists a unique stable synchronous solution to Eq. (9) for the levels of heterogeneity considered. In addition, once the synaptic strength has evolved within the region of 1:1 synchronous locking, iSTDP further modulates the synaptic strength such that it approaches monotonically to a final stable configuration wherein the two neurons are locked in in-phase 1:1 synchrony. We also demonstrated, the influence of the initial synaptic strength in achieving the final 1:1 in-phase synchronous solution.

We next show through numerical simulations, that the enhancement in synchronization persists for mutually coupled pair of neurons in the presence of increasing levels of heterogeneity. For both intrinsic heterogeneity through different external drive and extrinsic heterogeneity through different decay time of the synapse and different strength of self inhibition, iSTDP is able to maintain synchrony between the coupled neurons. Although not presented in this work, the stability of the synchronous state for the MCI can also be studied using the STRC method (Acker et al. 2004).

This effect of the iSTDP in enhancement of synchrony in the UCI and the MCI in the presence of heterogeneity in the firing rates of the two coupled neurons is an interesting result from neuroscience perspective as it suggests that neural system through STDP is very robust against any external perturbation and that system always phase locks in in-phase synchrony. While such a robust state of neural synchrony is essential for memory consolidation, it might not be an optimal scenario for sensory information processing wherein sensory information is encoded in the form of a temporal code and a robust neural synchrony might result in loss of all sensory information.

We have also done numerical simulations with mild noise in the intrinsic firing rate of each coupled neuron and the iSTDP rule to study the influence of noise in the coupled system on the synchrony induced by iSTDP. We found that the synchrony remains enhanced with iSTDP for all the levels of heterogeneity considered. However under similar noise conditions, synchrony is completely lost with static synapse. Details on the influence of iSTDP learning on synchrony in the presence of noise will be presented in the forthcoming work.

Higher frequency synchronous oscillations have been reported experimentally in behaving animals (Ylinen et al. 1995). Our study above suggest that iSTDP might in fact work better at such high frequencies, in maintaining synchronous network oscillations. It has been suggested in Haas et al. (2006), that plasticity of inhibitory synapses may play an important role in balancing the effect of excitatory synapse preventing run away behavior typically observed in epileptogenesis. Also recently Abarbanel and Talathi (2006), used the model for STDP used in this work to design a neural circuitry for spike pattern recognition. In this work we

present yet another important function for STDP in inhibitory synapses: its role in maintaining synchrony in networks of coupled interneurons, under biologically realistic situation of mild heterogeneity and noise.

Acknowledgements This work was performed under the sponsorship of the Office of Naval Research (Grant N00014-02-1-1019) and the National Institute of Health Collaborative Research in Computational Neuroscience program (1R01EB004752).

References

Abarbanel, H., Gibb, L., Huerta, R., & Rabinovich, M. (2003). Biophysical model of synaptic plasticity dynamics. *Biological Cybernetics, 89*, 214–226.

Abarbanel, H., & Talathi, S. (2006). Neural circuitry for recognizing interspike interval sequences. *Physical Review Letters, 96*, 148104.

Acker, C., Kopell, N., & White, J. (2004). Synchronization of strongly coupled excitatory neurons: Relating network behavior to biophysics. *Journal of Computational Neuroscience, 15*, 71–90.

Benardo, L. (1997). Recruitment of GABAergic inhibition and synchronization of inhibitory interneurons in rat neocortex. *Journal of Neurophysiology, 77*, 3134–3144.

Bragin, A., Jando, G., Nadasdy, Z., Hetke, J., Wise, K., et al. (1995). Gamma (40–100 Hz) oscillations in the hippocampus of the behaving rat. *Journal of Neuroscience, 15*, 47–60.

Eckhorn, R., Bauer, B., Jordan, W., Brosch, M., Kruse, W., et al. (1988). Coherent oscillations: A mechanism of feature linking in the visual cortex. *Biological Cybernetics, 60,* 121–130.

Ermentrout, B. (1996). Type 1 membranes, phase resetting curves and synchrony. *Neural Compute, 8*, 979–1001.

Ernst, U., Pawelzik, K., & Geisel, T. (1995). Synchronization induced by temporal delays in pulse-coupled oscillators. *Physical Review Letters, 74*, 1570–1573.

Froemke, R., & Dan, Y. (2002). Spike-timing-dependent synaptic modification induced by natural spike trains. *Nature, 416*, 433–438.

Gray, C., Koenig P, Engel, K., & Singer, W. (1989). Oscillatory responses in cat visual cortex exhibit intercolumnar synchronization which reflect global stimulus properties. *Nature, 338*, 334–337.

Haas, J., Nowotny, T., & Abarbanel, H. (2006). Spike-timing-dependent plasticity of inhibitory synapses in the entorhinal cortex. *Journal of Neurophysiology, 96*, 3305–3313.

Jefferys, J., Traub, R., & Whittington, M. (1996). Neuronal networks for induced 40 Hz rhythms. Trends in *Neuroscience, 19*, 202–208.

Kopell, N., & Ermentrout, B. (2004). Chemical and Electrical synapses perform complementary roles in the synchronization of interneuronal networks. *Proceedings of the National Academy of Sciences, 101*, 15482–15487.

Kurths, J., Pikovsky, A., & Rosenblum, M. (2001). *Synchronization, a universal concept in non-linear science.* Cambridge University Press.

Lacaille, J., & Williams, S. (1990). Membrane properties of interneurons in stratum oriens-alveus of the CA1 region of rat hippocampus in vitro. *Neuroscience, 36*, 349–359.

McCormick, D., Connors, B., Lighthall, J., & Prince, D. (1985). Comparative electrophysiology of pyramidal and sparsely spiny stellate neurons of the neocortex. *Journal of Neurophysiology, 54*, 782–806

Michelson, H., & Wong, R. (1994). Syncrhonization of inhibitory neurones in the guinea-pig hippocampus in vitro. *Journal of Physiology, 477*, 35–45.

Nowotny, T., Zhigulin, V., Selverston, A., Abarbanel, H., & Rabinovich, M. (2003). Enhancement of synchronization in hybrid neural circuit by spike timing dependent plasticity. *Journal of Neuroscience, 23*, 9776–9785.

Oprisan, S., Prinz, A., & Canavier, C. (2004). Phase resetting and phase locking in hybrid circuits of one model and one biological neuron. *Biophysical Journal, 87*, 2283–2298.

Ritz, R., & Sejnowski, T. (1997). Synchronous oscillatory activity in sensory systems: New vistas on mechanisms. *Current Opinion in Neurobiology, 7*, 536–546.

Sheperd, G. (1990). *The synaptic organization of the brain.* New York: Oxford University Press.

Skinner, F., Zhang, L., Velazquez, P., & Carlen, P. (1999). Bursting inhibitory interneuronal networks: A role for gap-junctional coupling. *Journal of Neurophysiology, 81*, 1274–1283.

Traub, R., Kopell, N., Bibbig, A., Buhl, E. H., le Beau, F., et al. (2001). Gap junctions between interneuron dendrites can enhance synchrony of gamma oscillatios. *Journal of Neuroscience, 21*, 9478–9486.

vanVreeswijk, C., Abbott, L., & Ermentrout, B. (1994). When inhibition and not excitation synchronizes neural firing. *Journal of Computational Neuroscience, 1*, 313–321.

Wang, X., & Rinzel, J. (1992). Alternating and synchronous rhythms in reciprocally inhibitory model neurons. *Neural Computation, 4*, 84–97.

White, A., Chow, C., Ritt, J., Trevino, C., & Kopell, N. (1998). Synchronization and oscillatory dynamics in heterogeneous, mutually inhibited neurons. *Journal of Computational Neuroscience, 5*, 5–16.

Whittington, M., Traub, R., & Jefferys, J. (1995). Synchronized oscillations in interneuron networks driven by metabotropic glutamate receptor activation. *Nature, 373*, 612–615.

Wilkie, J. (2004). Numerical methods for stochastic differential equations. *Physical Review E, 70*, 017701.

Woodin, M., Ganguly, K., & Poo, M. (2003). Coincident Pre- and Postsynaptic activity modifies GABAergic synapses by postsynaptic changes in Cl Transporter activity. *Neuron, 39*, 807–820

Ylinen, A., Bragin, A., Nadasdy, Z., Jando, G., Szabo, I., et al. (1995). Sharp wave-associated high-frequency oscillation (200 Hz) in the intact hippocampus: network and intracellular mechanisms. *Journal of Neuroscience, 15*, 30–46.

Zhigulin, V., Rabinovich, M., Huerta, R., & Abarbanel, H. (2003). Robustness and enhancement of neural synchronization by activity-dependent coupling. *Physical Review E, 67.*